XI International Conference on Computational Plasticity. Fundamentals and Applications
COMPLAS XI
E. Oñate, D.R.J. Owen, D. Peric and B. Suárez (Eds)

JOHNSON-COOK PARAMETER IDENTIFICATION FOR AISI-304 MACHINING THROUGH NELDER MEAD METHOD

C. M. GIORGIO BORT*, P. BOSETTI* AND S. BRUSCHI*

*Department of Mechanical and Structural Engineering (DIMS)
University of Trento
Via Mesiano 77, 38123 Trento, Italy
e-mail: dims@ing.unitn.it, www.unitn.it/en/dims

Key words: Orthogonal Cutting, Parameter identification, Johnson Cook, Nelder Mead Method

Abstract. The finite elements method (FEM) represents a useful tool for simulating machining processes, nevertheless numerical models are very sensible to the adopted material model and related constants. The paper reports a novel approach for the identification of the material parameters of the Johnson-Cook (JC) plasticity model, which is currently utilized in modeling material behavior during machining operations thanks to its capability to account for the material sensitivity to strain, strain rate, and temperature. The presented approach is based on the use of the Nelder Mead Method (NMM) to identify both the parameters of the simplified JC model and the friction factor of the Tresca law. NMM is a non-linear heuristic technique that affords to find local minima. Compared to the evolutionary approach typically used in parameter identification, the main benefit of this method consists in the low number of iterations necessary to achieve a good match between the experimental and numerical process outputs.
The reference process is the Orthogonal Tube Cutting (OTC) test of AISI 304 thin tubes. Although the AISI 304 is a well-known material and many data are available in literature, its reported JC parameters are characterized by a large dispersion, making necessary to develop a robust parameter identification procedure to have reliable material data to calibrate the numerical model.
OTC tests were carried out on an instrumented lathe and their numerical model developed through the commercial FEM software Deform^{TM} 2D v.10.1. The optimization problem was implemented in the language programming Ruby. The comparison between experiments and numerical results was made with regard to the cutting force, the tool-chip contact length, and the chip morphology.

1 INTRODUCTION

In the last decades, many efforts have been made in modeling machining processes, and different approaches have been used implying the development of statistical processes, theoretical and numerical models. Among the latter, the finite elements method (FEM) is the more utilized, since it is capable to handle a large number of process inputs and to represent as well several outputs, such as the temperature distribution in the workpiece, chip and tool, forces, chip morphology, residual stresses [1], and tool wear [2]. On the contrary, numerical models of machining operations can be computationally expensive and are highly sensible to the model parameters, especially as regards the rheological and tribological data. In machining operations the workpiece is in fact highly stressed in the primary and secondary shear zones, and it undergoes strains higher than 200 % at strain rates of more than 10^6 $1/s$. However rheological and tribological data are generally unknown at high strains and strain rates, therefore it is necessary to develop a robust strategy to identify these model unknowns.
The workpiece flow stress model commonly used for machining simulations is the Johnson-Cook constitutive equation [3]. It correlates the flow stress to the workpiece temperature, strain, strain rate, and is represented by the following equation:

$$\sigma(T, \epsilon, \dot{\epsilon}) = (A + B\,\epsilon^n)\left[1 + C\,ln\left(\frac{\dot{\epsilon}}{\dot{\epsilon}_0}\right)\right]\left[1 - \left(\frac{T - T_r}{T_m - T_r}\right)^m\right] \tag{1}$$

where T (^oC) is the workpiece temperature, T_m (^oC) the melting temperature, T_r (^oC) the room temperature, ϵ the plastic strain, $\dot{\epsilon}$ ($1/s$) the strain rate, A (MPa) the yield strength, B (MPa) and n the hardening modulus and the hardening coefficient respectively, C the strain rate sensitivity, and m the thermal softening coefficient. The friction model commonly used for machining simulations is the Tresca law due to high local pressure involved at the tool-workpiece contact. The Tresca law is represented by:

$$\tau = t\,\tau_{max} \tag{2}$$

where τ (MPa) is the tangential friction stress, τ_{max} (MPa) the maximum admissible tangential stress, and t the friction factor.

The reference process utilized in this paper for the identification of the Johnson Cook parameters is the Orthogonal Tube Cutting (OTC) test carried out on $AISI\,304$ thin tubes. The scientific literature reports different approaches for the identification of the Johnson Cook parameters of the stainless steel $AISI\,304$. Chandraserkaran *et al.* [4] demonstrated that the Split-Hopkinson pressure bar test can achieve a limited range of strains and, for this reason, this kind of test cannot be used in the parameter identification of the material model for machining processes. They stated that to identify the correct flow stress law at high strains and strain rates a combination between numerical simulations and experimental tests must be used. Lee *et al.* [5] combined quasi static and dynamic compressive tests with FEM simulations to fit the measured flow stress with the

Johnson Cook law, at three different strain rates, up to 10^3 $1/s$. Higher strain rates, up to 5×10^4 $1/s$, where achieved by Vural *et al.* [6] developing a new shear compression specimen. Nevertheless, even when modeling the same material, it is possible to find in literature that different sets of material parameters have been used in process simulations [7]-[9].
The sets of the JC parameters found in literature for the stainless steel AISI 304 were used in the FEM simulations of the OTC test, and a comparison between their outputs and the OTC results is presented in this study. The observable parameters are the cutting force, the chip thickness and curvature, and the tool-chip contact length. Very different results were obtained, proving that it is necessary to identify the material model parameters and the tribological factor through a more robust method. Shrot [11] utilized FEM machining simulations and the Levenberg-Marquardt optimization algorithm to identify the coefficients A, B and n of the equation 1. The hypotheses assumed in the Shrot's study deal with the process considered adiabatic and the neglection of the friction phenomena, which, however, can hardly describe the mechanical phenomena characterizing the real cutting processes.
The purpose of this work is to develop an approach dedicated to the simultaneous identification of the rheological and tribological parameters to be implemented in the numerical model of a machining operation. This is achieved by minimizing, through a customized Nelder Mead Method (NMM) [12], the sum square error between the calculated cutting force and chip morphology through FEM simulations, and those measured in an experimental OTC test. NMM is a simplex-based technique that can require a low number of iterations to converge to local minima, compared to the derivatives and evolutionary approaches typically used in parameter identification. On the contrary, NMM is highly sensible to the initial simplex, thus some considerations were made in choosing the starting simplex.

2 EXPERIMENTAL SET-UP

The OTC test consists on a rotating tube and a translating tool with a feed rate orthogonal to the cutting speed. The test was carried out on an industrial lathe (figure 1). The tube was made of $AISI\,304$, its external diameter was 50 mm and its wall 1 mm thick. The tool was made of high speed steel (HSS) with a TiN coating, its rake angle was $18° \pm 2°$ and its inclination angle zero. The process parameters were chosen accordingly to the data sheet given by the tool manufacturer, setting the cutting speed to 26,77 m/min, and feed rate to 0.09 mm/rev.
The chosen observables parameters were the cutting force, the chip thickness and curvature, and the tool-chip contact length. The force was measured by means of a Kistler™ multicomponent dynamometer $9257B$ placed below the toolholder (figure 1). The acquired average value of the cutting force was 182 N, identified at the attainment of the test steady state condition. The chip thickness and curvature were evaluated at the

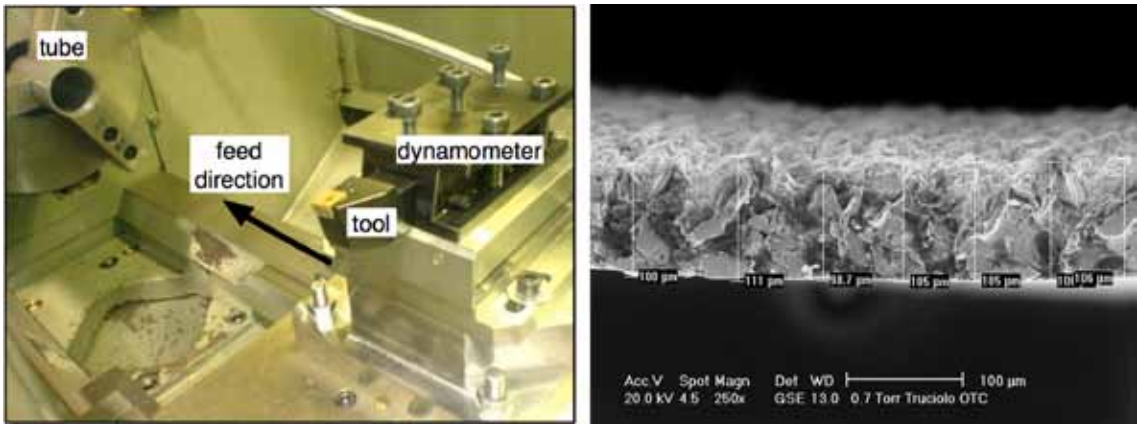

Figure 1: The experimental set-up used in the OTC test (left) and the measured chip (right).

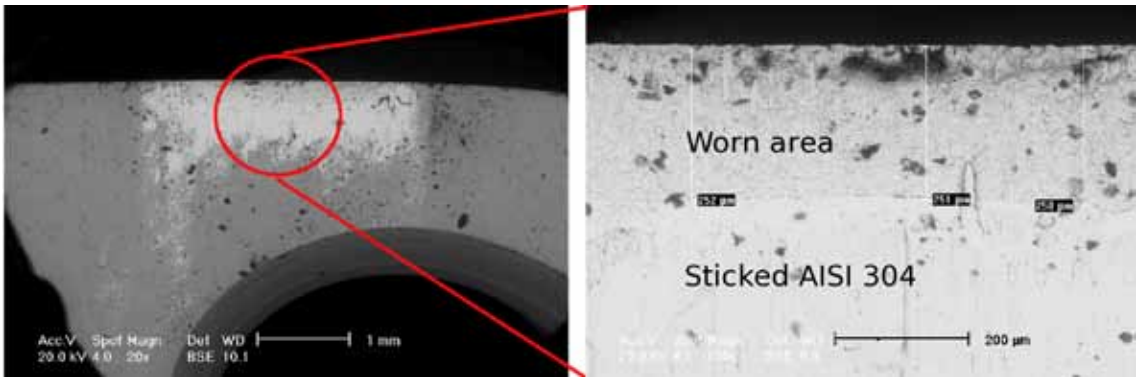

Figure 2: The tool flank at ESEM microscope (left) with a particular of the tool wear with the worn area and the $AISI\,304$ sticking zone (right).

ESEM microscope: seven different sections of the chip were considered measuring an average thickness of 105 μm, while the curvature radius was 1.51 mm^{-1}. Also the tool-chip contact length was measured at the ESEM microscope, by considering the tool wear after several cuts. In figure 2 it is possible to associate the clearest zone on the insert flank to the worn area. Focussing the attention to the wear zone, two different regions can be distinguished: the one nearest to the cutting edge is the real worn area in which the TiN coating has been removed, while the second one is evident due to the sticked $AISI\,304$ deposited during the cut. The latter is not a worn zone and for this reason is not considered in the measurements. The average chip contact length was 250 μm.

3 NUMERICAL MODEL

Due to the reduced feed rate compared to the thickness of the tube, it was possible to assume a plane strain condition for the above described machining process. A bi-dimensional

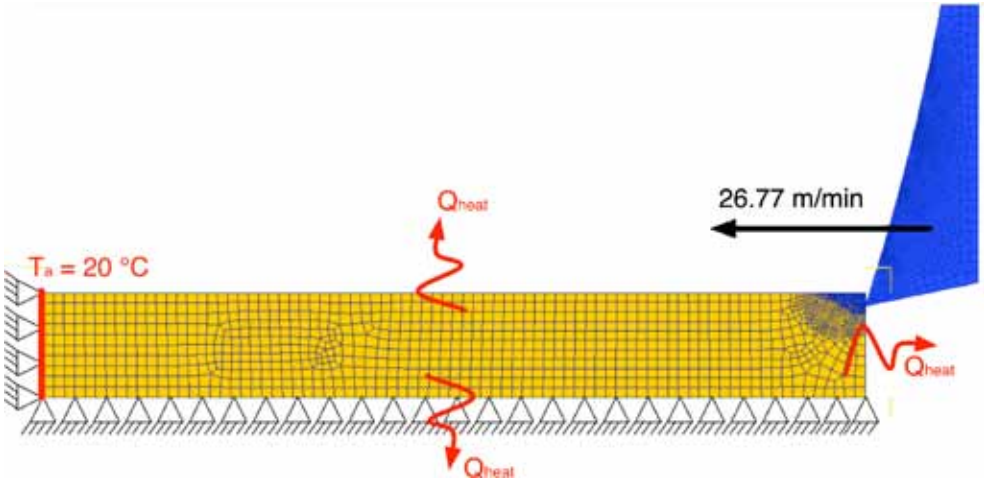

Figure 3: The OTC test model implemented in Deform^{TM} 2D.

numerical model was implemented in the commercial FEM software Deform^{TM} 2D (figure 3), which solves the thermo-mechanical problem using a Lagrange implicit method. The time step was set to 5 μs and the cutting length was 5 mm to ensure the achievement of the steady state condition. The process parameters were chosen accordingly to those used in the experimental test: depth of cut of 0.09 mm, cutting speed of 26,77 m/min, tool rake angle of 18°. The tool was considered as a rigid material and the workpiece as a plastic one since the residual stresses were not chosen as observables parameters.
An adaptive mesh was used, with tetrahedral quadratic elements. At the beginning of the simulation the workpiece was discretized with 1700 elements and the tool with 1600 elements, but due to the adaptive re-meshing, the number of the workpiece elements at the end of the simulation was approximately 3500. One finer mesh window was set on the workpiece moving together with the tool to have always an higher number elements in the workpiece zone nearest to the cutting edge: in this zone the length of the element edge was set to 6 μm. Null horizontal and vertical speeds were imposed at the workpiece's bottom and left edges. Moreover, the workpiece edge at left was considered at room temperature (i.e. 20°C) and the others exchanged heat with the environment or the tool. The convection coefficient was set equal to 10 $W/m^2\,K$. Accordingly to the literature review, the heat transfer coefficient between the workpiece and the tool was set equal to 3000 $W/m^2\,K$. The used friction model was the Tresca law by considering that in OTC, as it is for the machining processes, the real and the apparent contact areas between the chip and the tool are almost equal.
Two model features remain unknown and must be determined: the friction factor of the Tresca law, and the workpiece material parameters of flow stress law (i.e. the five material parameters of the JC model). The identification of these parameters was performed by using the optimization algorithm proposed in the next section.

3.1 Model sensitivity to JC parameters from literature

In order to analyze the model sensitivity to the rheological parameters, numerical simulations of the OTC test with the above described model were carried out by using the JC parameters found in literature for $AISI\,304$ and the experimental flow stress law implemented in the Deform^{TM}'s material library. The further parameters were used in modeling different processes with different strain rates. As it can be seen in table 1, the J-C parameters differ significantly from each other. For all the simulations, the friction factor was set equal to 0.9, representative of dry conditions [13].
The table 2 summarizes the results obtained with the simulations carried out. Due to the high percentage error associated to all the calculated observables, neither the set of parameters available in literature nor the data of the Deform^{TM}'s material library could be considered valid for developing a reliable numerical model.

Table 1: JC parameters for $AISI\,304$ from literature.

	Processes	Strain rates	A	B	C	n	m
Ocana	Pulse laser microforming	10^3	350	275	0.022	0.36	1.0
Aquaro [8]	Peen forming	$> 10^6$	239	522	0.1	0.65	0.63
Mori [9]	Impulsive loads	10^3	310	1000	0.07	0.65	1

Table 2: Results from the simulations carried out with the JC parameters from literature.

Output	Measurements	Ocana [7]	Aquaro [8]	Mori [9]	Deform
Cutting force $[N]$	182	118	394	425	238
Error %	-	35	116	133	31
Chip thickness $[mm]$	0.105	0.241	0.369	0.460	0.3348
Error %	-	129	251	338	219
Chip contact length $[mm]$	0.250	0.173	0.501	0.617	0.3259
Error %	-	308	100	147	219
Chip curvature $[1/mm]$	1.510	0.524	0.0	0.0	0.01
Error %	-	65	100	100	99

4 OPTIMISATION ALGORITHM

The block diagram 4 schematizes the optimization software architecture, which utilizes two programming environments: Ruby [14] and Deform^{TM} 2D. The further has been chosen in this study since it is an object-oriented programming language, it is freeware, and thanks to its capabilities in handling regular expressions and blocks it is possible to develop a compact-high efficient code. In the following section a brief introduction to the modified Nelder Mead Method (NMM) and to the processing procedure developed in Ruby is presented.

4.1 The modified Nelder Mead Method

The optimization is carried out through the Nelder Mead Method. This is a simplex method useful for local minimization and it was implemented in a simplified version. Typically, NMM starts from an initial simplex and moves the vertices, accordingly to its image value, in the direction of the minimum. Four different operations can be performed to change the vertices: reflection, expansion, contraction and shrink. At each minimization step, the centroid M of hyper-face opposed to the worst point and the reflected point R are computed through the equations 3 and 4 respectively:

$$M = \frac{\sum_{i=1}^{N} V_i}{N-1} \tag{3}$$

$$R = 2\,M - W \tag{4}$$

where V_k is the k-th vertex of the simplex with N vertices and W is the vertex with the highest image. The reflection consists in moving the worst vertex on the opposite side of the line between the two best vertices. The expansion acts as the reflection, but the new vertex is moved farther, and it is performed when the new reflected vertex is lower than the lowest point in the simplex. The expanded point E can be evaluated by:

$$E = 2\,R - M \tag{5}$$

If the reflected vertex is higher or equal than the worst point in the simplex, then a contraction is executed. The contracted point C_1 is equal to:

$$C_1 = \frac{W+M}{2} \tag{6}$$

The last possible condition is that the reflected point is higher than the second best vertex and lower than the worst vertex. If these conditions are satisfied, a different contraction is performed:

$$C_2 = \frac{W+R}{2} \tag{7}$$

In the presented algorithm the shrink was not implemented because this operation requires two evaluations of the target function at each optimization step. As a consequence, the convergence would become slower than for the standard method, even if the algorithm would require a lower number of simulations to achieve a satisfactory solution. The convergence criteria is based on the simplex norm, i.e. the sum of the differences of all possible combinations of vertices values.
In the developed numerical model, six unknowns have to be determined, meaning that the dimension of the simplex is seven. Since the solution found by NMM is strongly dependent from the first simplex choice, the first set of vertices was composed by the JC parameters found in literature [8]-[9] (with a friction factor t of 0.9) and others five points randomly chosen. The starting simplex is reported in table 3.

Table 3: The starting simplex used for the optimization.

Vertex No.	A	B	C	n	m	t
1	350	275	0.022	0.36	1.000	0.60
2	310	1000	0.070	0.65	1.000	0.50
3	1000	1500	0.014	0.36	1.000	0.90
4	239	522	0.100	0.65	1.000	0.70
5	129	85	0.023	0.97	0.458	0.40
6	784	812	0.459	0.51	0.196	0.69
7	649	1136	0.372	0.73	0.207	0.80

4.2 The optimization procedure

The main tasks performed by the Ruby Optimization Procedure (ROP) are to run the optimization and to interact with Deform^{TM} in batch mode, giving the chance to automate the pre-processing phase, simulation execution and post-processing analysis.
The output of the optimization step is a configuration file used as input for the numerical model. The ROP runs the pre-processor to generate the model database file, representing the numerical model. Then the ROP executes Deform^{TM} 2D and waits until the simulation comes to an end.
If no errors occur at the end of the simulation, the procedure extracts the nodal coordinates of the final geometry of the chip. Then the nodes on the external and internal chip edges are identified (figure 4). The chip thickness is estimated as the difference between the radius of the circumferences interpolating the points on external and internal chip edges. The mean radius between these two circumferences gives the chip curvature. The chip contact nodes are identified by the contact boundary condition applied on them, and they are used to calculate the tool-chip contact length. Finally, the cutting force

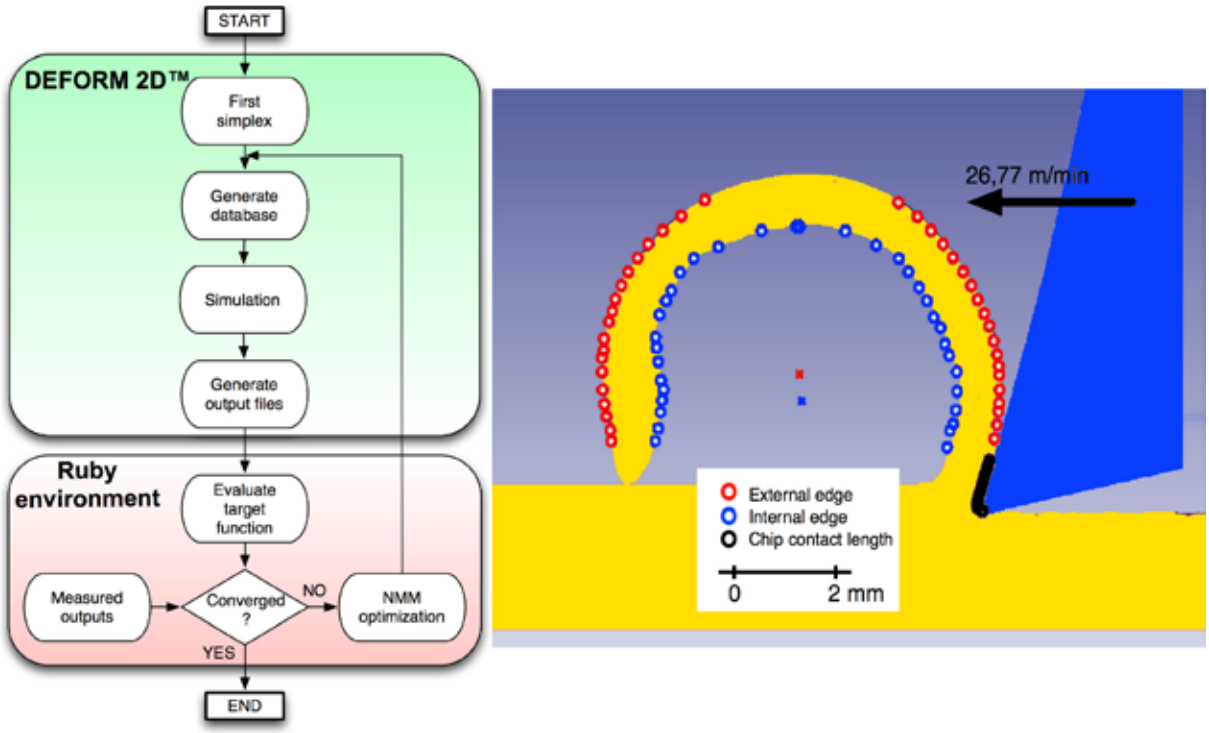

Figure 4: The scheme of the optimization software developed under Deform^{TM} 2D and Ruby environments (left). The identified chip contact nodes, external and internal edges (right).

is obtained by calculating the average of the cutting force values when the steady state conditions are reached. The target function is defined as the sum of the percentage error between the measured outputs and the calculated ones. Penalty functions are used to avoid negatives rheological and tribological parameters. Let Y_m and Y_c be the vectors of four elements containing respectively the measured outputs and the calculated ones, and let X be the vector of six elements with the optimized parameters, the target function can be evaluated as:

$$f(X) = \sum_{i=1}^{4} \frac{|Y_{mi} - Y_{ci}|}{Y_{ci}} + \sum_{j=1}^{6} min(0, X_i)^2 \tag{8}$$

The first term in the equation represents the percentage error, and the second one the penalty function applied to all the rheological and tribological parameters. The algorithm ends when the simplex norm is less than 10.

5 RESULTS

After 20 iterations the optimization algorithm converged to the solution, being the last norm of the simplex 1.18. The convergence plot is reported in figure 5, where it can be seen that the simplex norm tends to zero. In the same figure the comparison between

the measured cutting force and the calculated one is shown: the fitting is satisfactory expecially if it is compared with the results obtained with the sets of Johnson-Cook parameters reported in literature and with flow stress data of the Deform^{TM}'s material library (see table 1). Figure 6 shows a qualitative comparison between the experimental chip morphology and the numerically calculated one: the results are acceptable. The set of Johnson-Cook parameters of the best vertex is reported in table 4, while the outputs calculated with these parameters are in table 5.

Table 4: The optimized set of parameters.

A	B	C	n	m	t
740	630	0.28	0.53	0.26	0.61

Table 5: The outputs obtained with the optimized set of parameters.

	Cutting force $[N]$	Chip thickness $[mm]$	Chip contact length $[mm]$	Chip curvature $[1/mm]$
Measured	182	0.11	0.25	1.51
Calculated	197	0.13	0.12	2.01
Error %	8	20	51	33

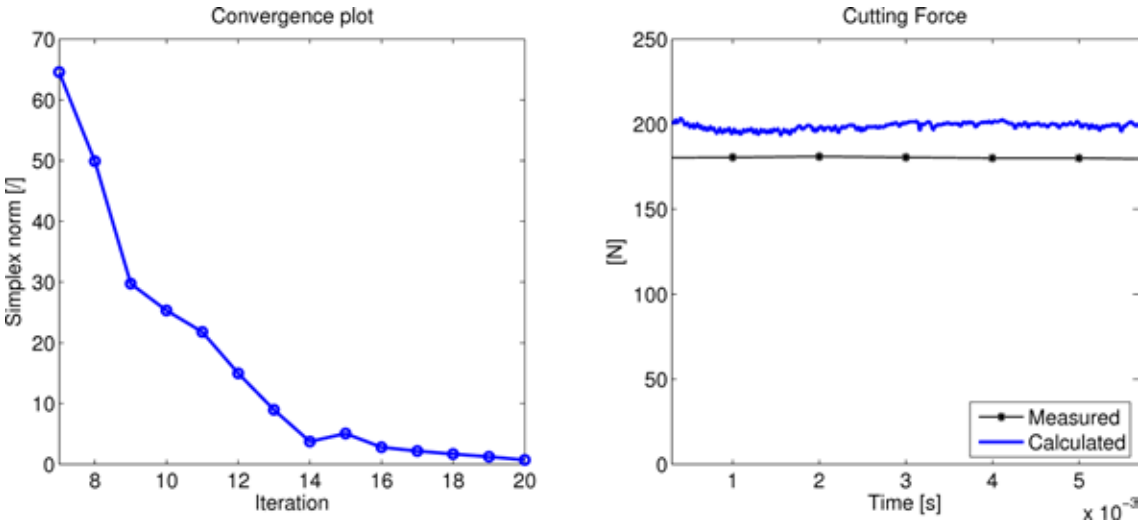

Figure 5: The convergence plot (left), the comparison between the measured cutting force and the calculated one (right).

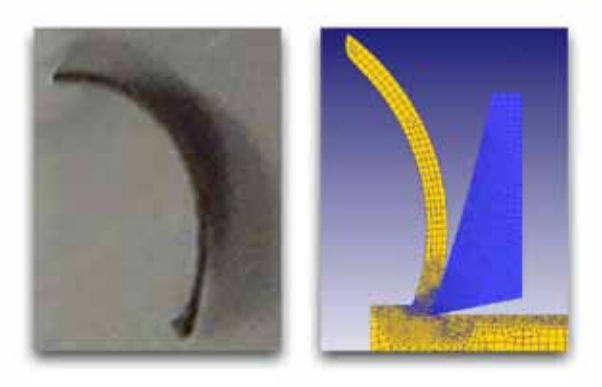

Figure 6: The measured chip (left) and the calculated one (right).

6 CONCLUSIONS

In this paper a numerical model of the orthogonal tube cutting test and a procedure for the material rheological parameters identification have been presented. The numerical model was developed in Deform^{TM} 2D and the optimization procedure was implemented in the programming language Ruby. The analyzed outputs were: the cutting force, the chip thickness and curvature, and the contact length between the tool and the chip. The coefficients of the Johnson Cook constitutive model and the friction factor of Tresca law were identified at the same time by minimizing the percentage error between the measured outputs and the calculated ones. Through the Nelder Mead Method, after 20 iterations, an optimal set of rheological and tribological parameters was found, and the calculated outputs were compared with experimental ones. The results can be considered acceptable compared to the ones obtained with sets of Johnson-Cook parameters available in literature. However, the evaluation of chip morphology is still not satisfactory: more analyses are going on to decrease the errors. Nevertheless, the developed approach can represent a useful tool in identifying the rheological behaviour of materials processed at high strain rates.

REFERENCES

[1] D. Umbrello, R. M'Saoubi and J.C. Outeiro, The influence of Johnson-Cook material constants on finite element simulation of machining of AISI 316L steel. *International Journal of Machine Tool & Manufacture* (2001) **47**:461–470.

[2] A. Attanasio, E. Ceretti and C. Giardini, 3D FEM simulation fo flank wear in turning. *Esaform proceedings* (2011), 561–566.

[3] G.R. Johnson and W.H. Cook, A constitutive model and data for metals subjected to large strains, high strain rate, and temperatures. **International Symposium on Ballistics** (1983), 1-7

[4] H. Chandrasekaran, R. MSaoubi and H. Chazal, Modelling of material flow stress in chip formation process from orthogonal milling and split Hopkinson bar tests. **Machining Science and Technology** (2005), **9**:131-145.

[5] S.Lee, F. Barthelat, J. W. Hutchinson and H.D. Espinosa, Dynamic failure of metallic pyramidal truss core materials Experiments and modeling. *International Journal of Plasticity* (2001), **22**:2118–2145.

[6] M. Vural, D. Rittel and G. Ravichandran, Large Strain Mechanical Behavior of 1018 Cold-Rolled Steel over a Wide Range of Strain Rates. **Metallurgical and materials transactions** (2003), **34A**:2873–2885.

[7] J.L. Ocaña, M. Morales, C. Molpeceres, O. Garca and J.A. Porro, J.J. Garca-Ballesteros, Numerical modelling and experimental characterization of short pulse laser microforming of thin metal sheets. **Multi-Material Micro Manufacture** (2008).

[8] D. Aquaro, Erosion rate of stainless steel due to the impact of solid particles. *AITC-AIT 2006 International Conference on Tribology* (2006).

[9] L. F. Mori, S. Lee, Z. Y. Xue, A. Vaziri, D. T. Queheillalt, K. P. Dharmasena, H. N. G. Wadley, J. W. Hutchinson and H. D. Espinosa, Deformation and fracture model os sandwich structures subjected to underwater impulsive loads. **Journal of mechanics of materuals and structures** (2007), textbf10:1981–2006.

[10] S. Y. Ahmadi-Brooghani, H. Hassanzadeh and P. Kahhal, Modeling of single-particle impact in abrasive water jet machinning. **World Academy of Science, Engineering and Technology** (2007), **36**:243–248.

[11] , A. Shrot and M. Bärker, How to identify Johnson-Cook parameters from machinning simulations. *Esaform proceedings* (2011), 29–34.

[12] J. H. Mathews and K. D. Fink, *Numerical methods using Matlab, 4^{th} Edition.* Prentice-Hall Inc., (2004), 430–436.

[13] C. M. Giorgio Bort, S. Bruschi and P. Bosetti, Modelling sawing of metal tubes through FEM simulation. *Esaform proceedings* (2011), 651–655.

[14] D. Thomas, *Programming Ruby, the pragmatic programmers' guide.* The Pragmatic Programmers, 2*nd* edition (2004).